

Pulse retrieval from interferometric autocorrelation measurement by use of the population-split genetic algorithm

Ching-Wei Chen, Jung Y. Huang and Ci-Ling Pan

*Department of Photonics and Institute of Electro-Optical Engineering, National Chiao Tung University
1001 Ta Hsueh Road, Hsinchu 30010, Taiwan, R.O.C.*

cwchen.eo90g@nctu.edu.tw, jyhuang@cc.nctu.edu.tw, clpan@faculty.nctu.edu.tw

Abstract: The population-split genetic algorithm (PSGA) was successfully applied to retrieve femtosecond optical fields from interferometric autocorrelation traces. PSGA strikes a balance between diversity and the size of population in the genetic algorithm. As a result, PSGA is less likely prematurely converging to sub-optimal solutions. Theoretical and experimental studies indicate that the PSGA can yield more accurate results in shorter time compared with conventional genetic algorithm and the iterative method.

©2006 Optical Society of America

OCIS codes: (320.7100) Ultrafast measurements; (320.5550) Pulses; (100.5070) Phase retrieval

References and links

1. K. W. DeLong, R. Trebino, J. Hunter and W. E. White, "Frequency-resolved optical gating with the use of second-harmonic generation," *J. Opt. Soc. Am. B* **11**, 2206-2215 (1994).
2. C. Iaconis and I. A. Walmsley, "Spectral phase interferometry for direct electric-field reconstruction of ultrashort optical pulses," *Opt. Lett.* **23**, 792-794 (1998).
3. J. -C. M. Diels, J. J. Fontaine, I. C. McMichael, and F. Simoni, "Control and measurement of ultrashort pulse shapes (in amplitude and phase) with femtosecond accuracy," *Appl. Opt.* **24**, 1270-1282 (1985).
4. J. W. Nicholson, J. Jasapara, W. Rudolph, F. G. Omenetto, and A. J. Taylor, "Full-field characterization of femtosecond pulses by spectrum and cross-correlation measurements," *Opt. Lett.* **24**, 1774-1776 (1999).
5. T. Hirayama and M. S. -Bahae, "Real-time chirp diagnostic for ultrashort laser pulses," *Opt. Lett.* **27**, 860-862 (2002).
6. D. A. Bender, M. P. Hasselbeck, and M. S. -Bahae, "Sensitive ultrashort pulse chirp measurement," *Opt. Lett.* **31**, 122-124 (2006).
7. D. J. Kane, "Real-time measurement of ultrashort laser pulses using principal component generalized projections," *IEEE J. Sel. Top. Quantum Electron.* **4**, 278-284 (1998).
8. R. Trebino, K. W. DeLong, D. N. Fittinghoff, J. N. Sweetser, M. A. Krumbiegel, B. A. Richman, and D. J. Kane, "Measuring ultrashort laser pulses in the time-frequency domain using frequency-resolved optical gating," *Rev. Sci. Instrum.* **68**, 3277-3296 (1997).
9. J. W. Nicholson, F. G. Omenetto, D. J. Funk, and A. J. Taylor, "Evolving FROGS: phase retrieval from frequency-resolved optical gating measurements by use of genetic algorithms," *Opt. Lett.* **24**, 490-492 (1999).
10. P. Honzatko, J. Kanka, B. Vraný, "Retrieval of the pulse amplitude and phase from cross-phase modulation spectrograms using the simulated annealing method," *Opt. Express* **12**, 6046-6052 (2004).
11. J. Peatross and A. Rundquist, "Temporal decorrelation of short laser pulses," *J. Opt. Soc. Am. B* **15**, 216-222 (1998).
12. J. W. Nicholson and W. Rudolph, "Noise sensitivity and accuracy of femtosecond pulse retrieval by phase and intensity from correlation and spectrum only (PICASO)," *J. Opt. Soc. Am. B* **19**, 330-339 (2002).
13. K. Naganuma, K. Mogi, and H. Yamada, "General method for ultrashort light pulse chirp measurement," *IEEE J. Quantum Electron.* **25**, 1225-1233 (1989).
14. M. C. Chen, J. Y. Huang, Q. T. Yang, C. L. Pan, "Freezing phase scheme for fast adaptive control and its application to characterization of femtosecond coherent optical pulses reflected from semiconductor saturable absorber mirrors," *J. of the Opt. Soc. Am. B* **22**, 1134-1142 (2005) and references therein.
15. X. Chu and S. -I. Chu, "Optimization of high-order harmonic generation by genetic algorithm and wavelet time-frequency analysis of quantum dipole emission," *Phys. Rev. A* **64**, 021403-1-021403-4 (2001).

16. I. Grigorenko, O. Speer, and M. E. Garcia, "Coherent control of photon-assisted tunneling between quantum dots: A theoretical approach using genetic algorithms," *Phys. Rev. B* **65**, 235309-1-235309-7 (2002).
 17. F. G. Omenetto, B. P. Luce, A. J. Taylor, "Genetic algorithm pulse shaping for optimum femtosecond propagation in optical fibers," *J. Opt. Soc. Am. B* **16**, 2005-2009 (1999).
 18. D. Zeidler, S. Frey, K. -L. Kompa, and M. Motzkus, "Evolutionary algorithms and their application to optical control studies," *Phys. Rev. A* **64**, 023420-1-023420-13 (2001).
 19. J. Kunde, B. Baumann, S. Arlt, F. M. -Genoud, U. Siegner, U. Keller, "Optimization of adaptive feedback control for ultrafast semiconductor spectroscopy," *J. Opt. Soc. Am. B* **18**, 872-881 (2001).
 20. R. Mizoguchi, K. Onda, S. S. Kano, A. Wada, "Thinning-out in optimized pulse shaping method using genetic algorithm," *Rev. Sci. Instruments*. **74**, 2670-2674 (2003).
 21. S. -F. Shu, Y. Lai, C. -L. Pan, "Learning evolution design of multiband-transmission fiber Bragg grating filters," *Opt. Eng.* **42**, 2856-2860 (2003).
 22. S. F. Shu, "Evolving ultrafast laser information by a learning genetic algorithm combined with a knowledge base," *IEEE Photon. Technol. Lett.* **18**, 379-381 (2006).
 23. S. F. Shu, C. L. Pan, and C. T. Sun, "Population-split genetic algorithm for retrieval of ultrafast laser parameters," *Int. J. Neural, Parallel, Sci. Comput.* **11**, 207-220 (2003).
 24. N. A. Campbell and J. B. Reece, *Biology* (Benjamin Cummings, San Francisco, 2002).
 25. Z. Michalewicz, *Genetic Algorithms + Data Structures = Evolution Programs* (Springer-Verlag, Berlin Heidelberg, 1996), Chap. 9.
-

1. Introduction

In order to generate and utilize ultrafast light pulses effectively, complete information about their optical field (amplitude and phase) must be available. A number of approaches to fully characterize femtosecond pulses from experimentally measurable quantities have been developed [1-7]. These include techniques such as the popular frequency resolved optical gating (FROG) [1] and spectral phase interferometry for direct electric-field reconstruction (SPIDER) [2]. For many applications, however, pulse-width and frequency chirp are monitored by simply taking the second-order interferometric autocorrelation (IAC) trace [3]. A related technique, phase and intensity from correlation and spectrum only (PICASO) was proposed and demonstrated to characterize ultrashort pulses without any time ambiguity [4]. More recently, the modified-spectrum autointerferometric correlation (MOSAIC) was developed to measure ultrashort pulse chirp [5,6].

Retrieval algorithms are required to extract complete phase information for all the above techniques. SPIDER utilizes, for example, a noniterative inversion routine that directly retrieves the phase from data by a series of linear transformations [2]. FROG, on the other hand, typically reconstructs pulse information by using an iterative algorithm based, for example, on the method of generalized projections [7], although a number of other algorithms and a composite algorithm have also been described [8]. In the case of second harmonic generation (SHG) FROG, Nicholson, *et al.* [9] showed that the genetic algorithm (GA) returned a lower error than the standard iterative composite algorithm. Other retrieval techniques, such as simulated annealing, have been demonstrated for retrieval of the pulse amplitude and phase from cross-phase modulation spectrograms [10]. With the reconstruction of the intensity profile from the autocorrelation trace, the Gerchberg-Saxton algorithm can be used to retrieve the phase of the electric field from a spectral measurement [11]. Several search algorithms, a simplex method, Powell's method and GA have been found suitable for PICASO [12]. Bender *et al.* [6] employed an improved real-time Fourier-transform algorithm [13] for MOSAIC. Previously, we reported a freezing phase algorithm (FPA) for adaptive coherent control and optical field characterization with a single apparatus [14].

It is highly desirable to have an efficient phase-retrieval algorithm with fast searching speed, high accuracy, and sufficient flexibility. Genetic algorithm, which is a global searching method based on ideas extracted from biological evolution, possesses advantages such as flexible searching ability and low likelihood to prematurely converge at a sub-optimal solution. The basic idea is that individuals with high fitness are the likely survivors in a challenging environment. During the evolution, the genetic information coded in the chromosomes can be changed by genetic operators such as crossover and random mutation.

In ultrafast-optics-related applications besides pulse characterization, a GA-based adaptive control scheme has been employed to investigate the quantum evolution of complex systems [15-17]. GA had been successfully employed to tailor a coherent optical field for preparing specific quantum states on the basis of fitness information [18, 19]. Nonetheless, GA has several shortcomings: Its trial-and-error procedure often leads to long convergence time. It is also prone to stall on a local extremum. GA must also be implemented with a sufficiently large population to preserve diversity. A “thinning-out” GA method was proposed and demonstrated for improving the convergence speed of a GA-based optimization of the pulse shaping technique [20]. We also showed learning GA evolves more quickly to more accurate designs of multiband-transmitting Bragg grating filters [21]. It was used to retrieve ultrafast laser pulse parameters from a simulated SHG-FROG trace [22]. The population-split genetic algorithm (PSGA) reported in our previous work [23] was used as a tool for evolution. It is shown that PSGA can yield more accurate solution in shorter period by using a smaller population size. The idea of population-split genetic algorithm (PSGA) originates from the yeast’s strategy during evolution. Yeast usually takes asexual reproduction to rapidly adapt in a benign environment, while it uses sexual reproduction to reproduce the offspring of different beneficial genotypes. This improves yeast’s probability of survival in a harsh environment [24].

From an experimental point of view, one of the simplest and most practical techniques for pulse retrieval is the measurement of the first-order and second-order interferometric correlation traces. In this paper, we apply PSGA to retrieve femtosecond optical fields from interferometric autocorrelation traces. PSGA strikes a balance between diversity with the size of population in genetic algorithm. Theoretical and experimental studies indicate that the PSGA can yield more accurate results in shorter time compared with conventional genetic algorithm and iterative method.

2. Methods

The structure of the PSGA algorithm is illustrated in Fig. 1.

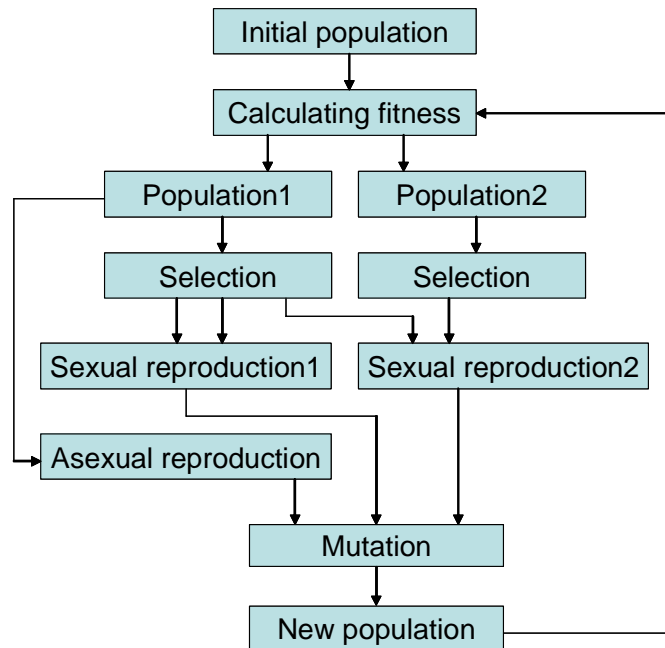


Fig. 1. Schematic of the structure of the PSGA algorithm

In each generation, typical genetic operators such as selection, crossover and mutation are used. As in conventional GA, PSGA employs a reproduction operator to emulate natural reproduction. Further, inspired by the yeast's strategy of rapid adaptation in a benign environment, PSGA allows the individuals with high-fitness to transmit their genes via asexual reproduction. To improve the survival probability in a harsh environment, PSGA also implements sexual reproduction to reproduce the offspring of different beneficial genotypes [24].

We have conducted a comparative study of PSGA, conventional GA, and iteration algorithm for pulse retrieval from interferometric autocorrelation measurements. Our procedure for phase retrieval from IAC is similar to that reported by K. Naganuma [13]. Input data are three Fourier moduli $|E(\omega)|_M$, $|I(\omega)|_M$, and $|U(\omega)|_M$ obtained from Fourier transformations of the measured autocorrelation functions $|G_I(\tau)|$, $|G_2(\tau)|$, and $|F_{SH}(\tau)|$, where the subscript, M, stands for measured values. $|G_I(\tau)|$ denotes the electric field autocorrelation function; $G_2(\tau)$ and $F_{SH}(\tau)$ are the intensity autocorrelation and second-harmonic field autocorrelation functions, respectively. The amplitude and phase of the pulse are retrieved iteratively according to the flow chart shown in Fig. 2:

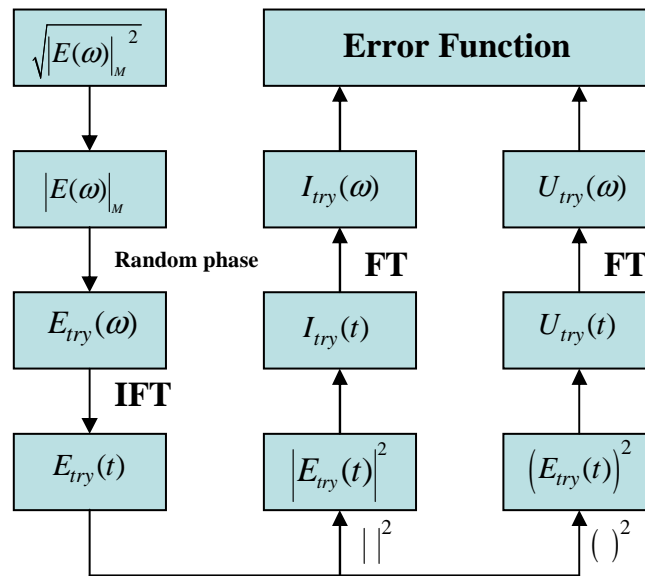


Fig. 2. Flowchart for phase retrieval of ultrafast pulses from IAC using PSGA.

To begin with, an initial trial function in the frequency domain is prepared by assigning random phases to the given $|E(\omega)|_M$ from the square root of the experimentally measured spectrum, $|E(\omega)|_M^2$. The trial profile of the optical pulse in the time domain, $E_{try}(t)$ can then be derived by the inverse Fourier transform of $E_{try}(\omega)$. By taking the squares of $|E_{try}(t)|$ and $E_{try}(t)$, $I_{try}(t)$ and $U_{try}(t)$ are obtained. The new power spectra of the fundamental and second-harmonic pulses $I_{try}(\omega)$ and $U_{try}(\omega)$ are just the inverse Fourier transform of $I_{try}(t)$ and $U_{try}(t)$.

As the phase retrieval loop proceeds, the trial function is iteratively refined. The errors in power spectra of the fundamental and second-harmonic signal, Z_I and Z_U , are defined to be the root-mean-square deviations of $I_{try}(\omega)$ and $U_{try}(\omega)$ from the measured spectral profiles. The error function Z (or its inverse the fitness function) can then be conveniently defined as

$$Z = \sqrt{Z_I^2 + Z_U^2} \quad (1)$$

$$Z_I^2 = \frac{\sum (|I_{try}(\omega)|^2 - |I(\omega)|_M^2)^2}{\sum |I(\omega)|_M^4} \quad (2)$$

$$Z_U^2 = \frac{\sum (|U_{try}(\omega)|^2 - |U(\omega)|_M^2)^2}{\sum |U(\omega)|_M^4} \quad (3)$$

Both the conventional GA and PSGA use a real codification with each real number corresponding to one spectral phase component of the electric field. In a typical run, a population of 18 individuals with different chromosomes is prepared. For phase retrieval of ultrafast pulses, the phase information of the optical pulse with squares of Fourier moduli $|E(\omega)|_M$, $|I(\omega)|_M$, and $|U(\omega)|_M$ are coded by 101 spectral components. A single chromosome represents a potential solution to the phase retrieval problem with an accuracy revealed by the error function. Therefore, each chromosome shall consist of 101 genes.

For PSGA, the population is split into two subgroups according to the error function. The chromosomes with first four lowest errors (or higher fitness) are grouped into population 1 and the remaining 14 chromosomes are assigned to population 2. Any individual in population 1 is allowed to carry on the asexual reproduction. Sexual reproduction, which exchanges the genetic information between two individuals, is implemented with a non-uniform arithmetical crossover operator [25] and is allowed either within population 1 or between the two populations. For the selection process, a roulette wheel with slots size proportional to the fitness is used (*i.e.*, the larger the fitness value is, the more likely it would be chosen). The mutation operator provides further random background variation in the components of the genes. Error function is evaluated for each produced offspring. The 18 individuals with the lowest values of error function are preserved for the next generation.

We have tested the PSGA with mutation rate, P , in the range of 0.01~0.1. Best performance was achieved with $P \approx 0.03$. That is, every gene has a probability of 3% to mutate. In other words, 3 genes will mutate if there are 101 genes in one chromosome. Generally speaking, two kinds of mutations are possible: uniform mutation (P_{um}) and non-uniform mutation (P_{nm}), for which the mutation rates are set to be $P_{um} = 0.025$ and $P_{nm} = 0.005$, respectively, with $P = P_{um} + P_{nm} = 0.03$. For uniform mutation, the genes are assigned a random number ranging from $-\pi$ to $+\pi$. For non-uniform mutation, an additional value of $\Delta(t,y) = y.r.[1-(t/T)]$ is added or subtracted from the random number. The parameter “y” is one of the operators responsible for fine tuning capabilities of the PSGA algorithm. It is defined such that the function $\Delta(t,y)$ returns a value in the range $[0, y]$ ensuring the probability of $\Delta(t,y)$ being close to 0 increases as t increases. This property causes the “y” operator to search the space uniformly initially (when t is small), and very locally at larger stages. In this work, y typically has the value 0.06; r is a random number lying in the range $[0, 1]$; t denotes the current number of generations for mutation; and T the total number of generations. The mutation operator can prevent PSGA from stalling at a local extremum. However, in order to guarantee fast convergence, the best chromosome is always preserved for the next generation.

In order to conduct a fair comparison, the same parameters, such as roulette wheel selection, non-uniform arithmetical crossover operator and uniform ($P_{um}= 0.025$) and non-uniform ($P_{nm}= 0.005$) mutation, respectively, are used in both conventional GA and PSGA.

3. Results and discussion

An asymmetric pulse with a higher-order chirp in its phase profile is employed to test the performance of different algorithms. The pulse is generated in the time-domain using the expression

$$E(t) = \exp[i\Psi(t)] * (A \cdot \exp[-(\frac{t-t_1}{T})^2] + B \cdot \exp[-(\frac{t-t_2}{T})^2]) \quad (4)$$

with a temporal phase profile

$$\Psi(t) = a(\frac{t}{T})^2 + b(\frac{t}{T})^3 + c(\frac{t}{T})^4 \quad (5)$$

where the parameters for the test pulse are as follows: $A = 0.7$, $B = 1$, pulse duration $T = 50$ fs, peak positions $t_1 = 45$ fs, $t_2 = 45$ fs, and $a = -0.1$, $b = -0.09$, $c = 0.01$.

Figure 3(a) shows the electric field profiles retrieved by PSGA, conventional GA, and iterative algorithm, respectively. For the same target pulse, we find that the PSGA yields a solution with an error as small as 0.00125, while GA and iterative algorithm generate results with an error of 0.03266 and 0.11061, respectively. Figure 3(b) depicts the errors of different algorithms as a function of generation number from 0 to 1000. As we can see, PSGA has reached a solution with an error $10^{-3} \sim 10^{-2}$ in 300 generations, while GA and iteration either requires much larger number of generations or is trapped at a suboptimal solution with larger error. For PSGA, the selection pressure built up from the selection process for sexual reproduction within the population 2 is similar to that in conventional GA. But the selection pressure from the asexual reproduction within the population 1 and the selection process for sexual reproduction between the populations 1 and 2 are unique for PSGA. This additional selection pressure in PSGA may be the driving force to yield the optimal solution in shorter time.

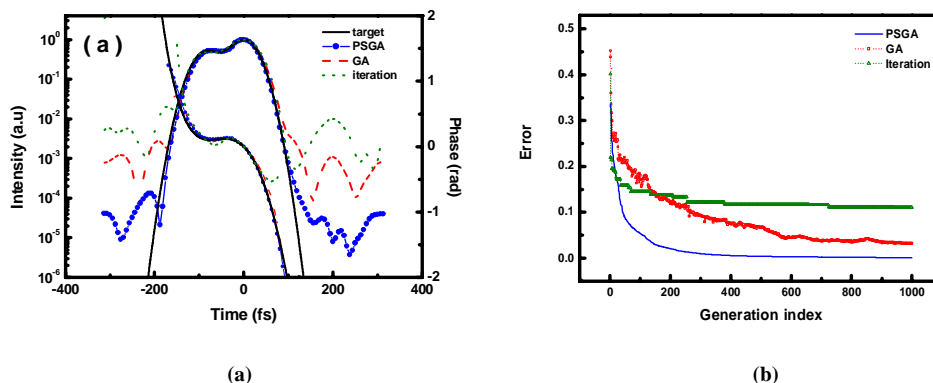


Fig. 3. (a) The target and the retrieved pulse intensities (log plot) and phases of a double-peaked pulse with complicated phase. (b) Error as a function of generation number for PSGA, conventional GA and iterative algorithms.

The two-dimensional plots shown in Fig. 4(a) for PSGA and Fig. 4(b) for GA present the dynamic distribution of genes with the x-axis denoting the 101 genes (*i.e.*, the spectral components of the optical pulse) and y-axis representing the 18 chromosomes (*i.e.*, the different potential solutions to the phase retrieval problem).

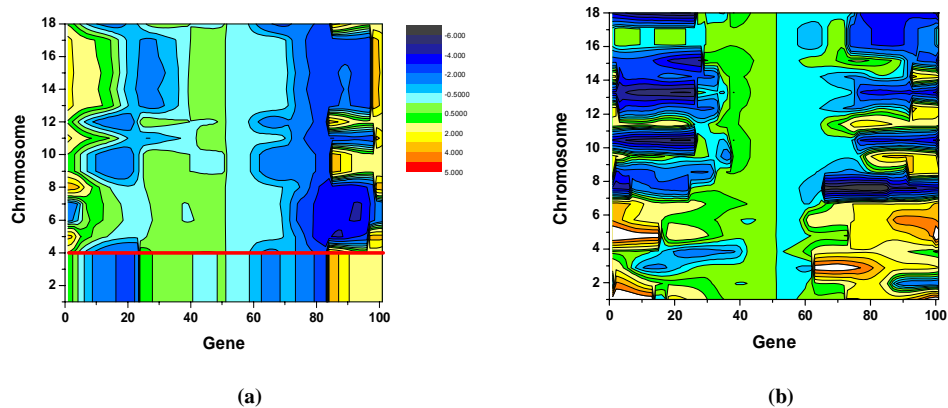


Fig. 4. Dynamic distributions of Genes at generation #3 for (a) PSGA and (b) conventional GA. The red line in Fig. 3(a), which marks the population splitting boundary, separates a region with much regular genetic organization from that with disordered genetic arrangement.

We order the chromosomes from 1 to 18 based on their fitness values. Chromosome 1 denotes the retrieved result with best fitness while chromosome 18 is the poorest one. The color coding shows the temporal phases retrieved by the algorithm used. Random phases are used as the initial guess for both PSGA and GA. Therefore, the dynamic distribution of the genes shall appear random in the two-dimensional plot at the beginning. We select generation #3 to illustrate the genetic distribution at the very early stage of phase retrieval for PSGA and GA. The red line in Fig. 4(a), which marks the population splitting boundary, clearly separates a region with much regular genetic organization from that with disordered genetic arrangement. The more ordered genetic distribution in the region of chromosomes 1 to 4 in Fig. 4(a) originates from the combined operation of asexual and sexual reproductions. In the early generations, the chromosomes 1~4 from asexual reproduction can guarantee the fast convergence; the remaining chromosomes 5~18 from sexual reproductions will preserve the high diversity for next generations to avoid the premature convergence. Compared with the result at generation #1000, the steady state phase profile in this region can achieve a root-mean-square (rms) error of 0.19 if genes with non-zero spectral intensity only are considered. In contrast, the genetic distribution of phases by conventional GA shown in Fig. 4(b) remains irregular. The difference of the two approaches is particularly striking for those genes with lower spectral intensity.

The comparison clearly indicates that PSGA, which specifically splits the populations and efficiently preserves the genetic information with better fitness, provides desirable features such as faster convergence and higher accuracy. Further, we note that PSGA works exceptionally well in retrieving asymmetric pulse with complicated phase profile while using a fairly small population size. It is well known that for GA, increasing the population size will increase the accuracy of phase retrieval while increasing population size causes the number of generations required for converging to increase. Small population size corresponds to less diversity and often causes GA to prematurely converge to sub optimal solution. In our problem the number of genes is as large as 101. The conventional GA with a population size of only 18 indeed prematurely converges to a sub optimal solution with a much higher error.

We further apply the three algorithms to analyze experimentally measured IAC traces in order to verify the superior performance of PSGA in practice. The IAC traces used were measured with a linear/second-order interferometric-type autocorrelator. The optical pulses are from a mode-locked Ti: sapphire laser with pulse duration of $\tau = 25$ fs at 90 MHz. Figures 5(a) and 5(b) show the measured linear and second-order interferometric autocorrelation traces.

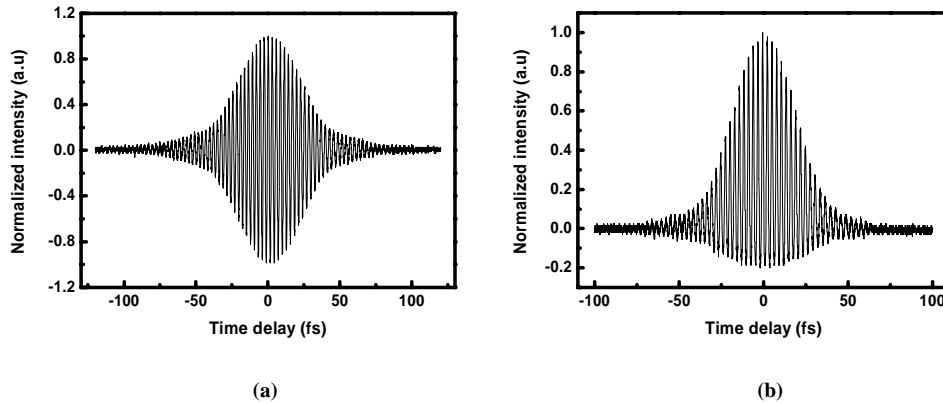


Fig. 5. Measured (a) linear (b) second-order interferometric autocorrelation traces of a 25-fs pulse train at 90 MHz.

Figure 6(a) exhibits the intensity and phase profiles of the pulses retrieved from the correlation curves shown in Figs. 5(a) and 5(b). The intensity and the phase profiles deduced from PSGA are plotted as the solid curve. The results from the conventional GA and iteration method are shown as the dashed and the dotted curves, respectively. Figure 6(b) summarizes the performance of PSGA, conventional GA, and iterative algorithm. The PSGA rapidly generates a solution with an error of 0.02833, the conventional GA and iterative method can only yield sub optimal results with error as large as 0.212 and 0.332.

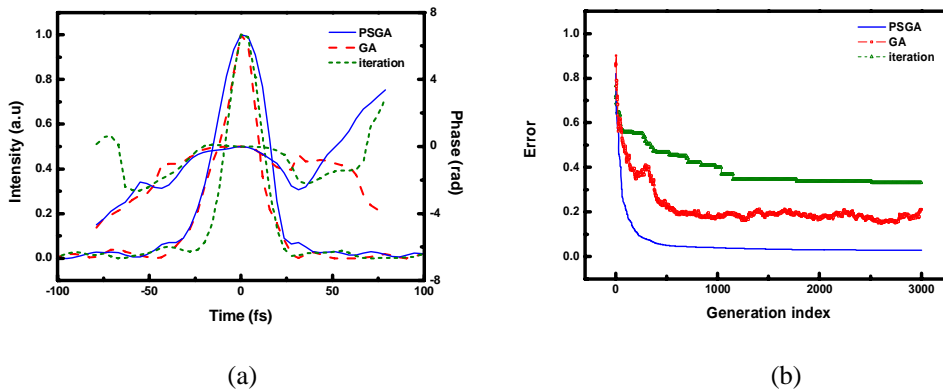


Fig. 6. (a) Intensity and phase of a 25-fs pulse train at 90 MHz retrieved by three different algorithms from target interferometric traces shown in Fig. 5. (b) Errors in the retrieved interferometric traces are plotted as a function of generation number for PSGA, conventional GA and iterative algorithm.

In the case of pulse retrieval from experimental data, experimental error and measurement noise are always a major concern. To minimize the effect of noise, data preprocessing is indispensable. Various data preprocessing had been employed in previous studies [12]. In this work, we first subtract the background from the profile of the spectral Fourier moduli and smoothly paddle the wings to zero. Then the retrieval error could be dramatically improved from 0.334 to 0.02833. Using the electric field retrieved from this preprocessed data, we found the pulse retrieval error to be much lower. The result is also more reproducible.

The retrieved amplitude and phase profiles can be used to calculate the second-order interferometric autocorrelation trace, which is shown as the solid curve in Fig. 7.

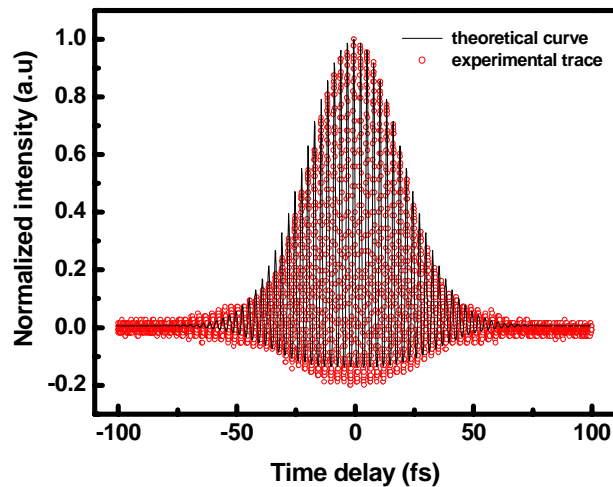


Fig. 7. Comparison between the experimental and theoretical second-order interferometric autocorrelation traces.

The open circles shown are the experimental trace, which agree well with the calculated curve. This result strongly supports that the retrieved information about amplitude and phase profiles by PSGA are fairly reliable and accurate.

We note that PSGA combined with interferometric autocorrelation technique will faithfully retrieve the phase information of optical pulses with fast convergence and high accuracy. Typically, the retrieval time is less than ten seconds for this algorithm running up to 1000 generations. In fact, the PSGA combined with FROG technique has also been performed in our lab. For the same FROG spectrograms, PSGA yields better performance than phase retrieval using either GA, or generalized projections, or Singular Value Decomposition (SVD) methods. However, due to a variety of the data sets of the FROG spectrograms, it is much time-consuming for algorithms to retrieve a reliable result than the case of IAC. Using PSGA in FROG, the retrieval usually takes several minutes to converge to a solution with low error.

4. Conclusions

In summary, we have demonstrated a new genetic algorithm with population splitting technique. This algorithm was applied to retrieve complete phase information of femtosecond pulses from measured interferometric autocorrelation traces. The PSGA exhibits several attractive features such as fast searching speed and high accuracy achieved with much smaller population size than the conventional GA. We expect that PSGA can also be a versatile tool for applications including optimal design of photonic devices, pulse shaping and ultrafast spectroscopy.

Acknowledgments

The authors acknowledge gratefully the support of National Science Council of the Republic of China under various grants as well as the Ministry of Education ATU program. The algorithm was compiled by Mr. Wen-Jr Jiang.